AGU PUBLICATIONS

Geochemistry, Geophysics, Geosystems

RESEARCH ARTICLE
10.1002/2014GC005325

Key Points:
- We determine relative vertical axis rotations within the island of Sardinia
- Breakup of Sardinia in at least two blocks after dyke emplacement
- Rotations can be due to Permian large-scale intra-Pangea wrench faulting

Correspondence to:
K. Aubele,
aubele@geophysik.uni-muenchen.de

Citation:
Aubele, K., V. Bachtadse, G. Muttoni, and A. Ronchi (2014), Paleomagnetic data from Late Paleozoic dykes of Sardinia: Evidence for block rotations and implications for the intra-Pangea megashear system, *Geochem. Geophys. Geosyst.*, *15*, 1684–1697, doi:10.1002/2014GC005325.

Received 6 MAR 2014
Accepted 27 MAR 2014
Accepted article online 1 APR 2014
Published online 2 MAY 2014

Paleomagnetic data from Late Paleozoic dykes of Sardinia: Evidence for block rotations and implications for the intra-Pangea megashear system

K. Aubele[1], V. Bachtadse[1], G. Muttoni[2], and A. Ronchi[3]

[1]Department of Earth and Environmental Sciences, Ludwig-Maximilians-Universität München, Munich, Germany, [2]Dipartimento di Scienze della Terra, Università di Milano, Milan, Italy, [3]Dipartimento di Scienze della Terra, Università di Pavia, Pavia, Italy

Abstract Paleomagnetic studies of dyke swarms from the Variscan belt of Europe can be used to reconstruct internal postorogenic rotations within the fold belt. Here we present paleomagnetic data from 13 late Variscan dykes from Sardinia ranging in age from 298 ± 5 to 270 ± 10 Ma. The dykes can be grouped on the basis of their different directions in strike in a northern, a central-eastern and a south-eastern province. Paleomagnetic component directions have been obtained using thermal and alternating field demagnetization techniques, which give reproducible results. The paleomagnetic mean directions differ significantly between northern Sardinia and south-eastern and central-eastern Sardinia, the latter two regions yielding statistically similar paleomagnetic mean directions. These results indicate that Sardinia fragmented into two, arguably three, crustal blocks after emplacement of the dykes, which experienced differential relative rotations, as is also indicated by the differences in overall strike directions. The determination of timing, sense, and magnitude of these rotations has major implications for the reconstruction of the geodynamic evolution of the region in post-Carboniferous times. We argue that the observed block rotations occurred during the Permian as the result of post-Variscan intra-Pangea mobility possibly related to the transformation of an Early Permian Pangea B to a Late Permian Pangea A.

1. Introduction

It has been previously observed that the use of paleomagnetic data to reconstruct Pangea A (Wegenerian Pangea) in the Early Permian results in a significant continental overlap of Laurasia and Gondwana, and that one of the options to overcome this problem is to choose an alternative configuration known as Pangea B, characterized by the southern continents of Gondwana located further to the East with respect to Laurasia [*Irving*, 1977; *Morel and Irving*, 1981; *Muttoni et al*., 2003; see *Aubele et al*. [2012] and *Domeier et al*. [2012] for a discussion of the Pangea controversy). However, since there is no reason to doubt that the opening of the Atlantic Ocean and the dispersal of Pangea started from a Pangea A configuration, a large dextral megashear zone between Laurasia and Gondwana becomes a necessary feature for the transformation from a postulated Pangea B to a widely accepted Pangea A configuration (Figure 1). Based on a variety of geological evidence [e.g., *Arthaud and Matte*, 1977; *Burg et al*., 1994; *Stampfli*, 2001; *Casini et al*., 2012], this tectonic zone, if real, is expected to lie within the Mediterranean realm in southern Europe and/or northern Africa.

According to *Irving* [1977], transform motion involved ∼3000 km of diffuse dextral shear. *Muttoni et al*. [2003] constrain the timing of transform motion to a ∼20 Ma interval during mid-Permian times, requiring an average relative plate velocity of ∼15 cm/yr. The driving force couple for the dextral motion of Gondwana relative to Laurasia was provided by (i) Neotethyan rifting along the eastern margin of Gondwana and (ii) the subduction of Panthalassan oceanic crust underneath the western margin of Gondwana. The existence of the postulated Pangea megashear system is therefore intimately coupled with important geodynamic processes during the Permian.

It has been postulated earlier that the tectonic inventory of relatively small crustal blocks including SE France, Corsica, and Sardinia could represent the remnants of a diffuse dextral plate boundary between Laurasia and Gondwana [*Aubele et al*., 2012]. Such crustal blocks caught within shear zones may exhibit differential vertical axis rotations, which can be quantified using paleomagnetic techniques as described in this study.

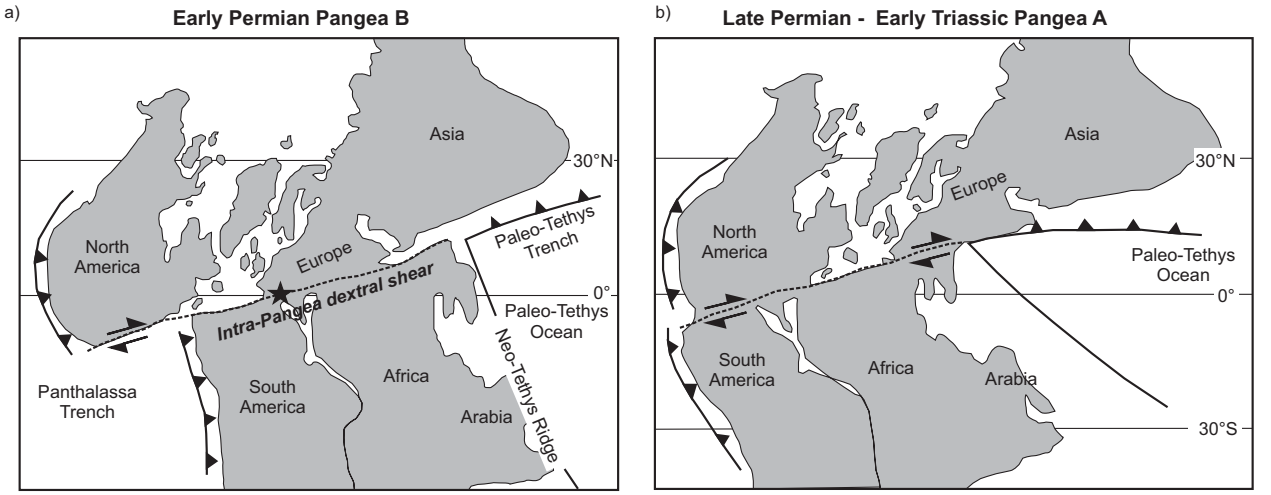

Figure 1. (a) Pangea B configuration after *Irving* [1977] in the early Permian. Star: approximate location of the study area. (b) Wegenerian Pangea A configuration in the Late Permian to Early Triassic. Modified after *Muttoni et al.* [2009].

The late Variscan Corsica-Sardinia Batholith is cut from north to south by an impressive dyke swarm; several dykes also cut the Variscan metamorphic basement as well as nonmetamorphic Permian volcanic rocks [e.g., *Traversa et al.*, 2003]. Two—arguably three—dyke provinces can be identified based on strike directions. If these strike differences are of tectonic origin, the crustal coherence of Sardinia as a single block, which has been proven valid since the Jurassic [*Kirscher et al.*, 2011], can no longer be maintained for pre-Jurassic times. This opens the possibility—explored in this paper—that these dykes were variably rotated shortly after emplacement and could represent evidence of Permian shearing between Laurasia and Gondwana.

The aim of this study is therefore to investigate whether the different strike directions of Sardinian dykes are of primary or secondary origin in order to quantify internal rotations within Sardinia and their implications for the inferred Pangea megashear system.

2. Geological Setting and Geochronological Data

Until the opening of the Gulf of Lyon during the Oligocene, the Corsica-Sardinia microplate was part of the southern margin of the European Variscides composed of metamorphic rocks of Early Cambrian to Early Carboniferous age that were deformed during the collision between Gondwana and Laurasia, as well as a late orogenic magmatic complex emplaced during a Late Carboniferous-Permian extensional phase [*Cortesogno et al.*, 1998; *Funedda and Oggiano*, 2009].

According to *Carmignani et al.* [1978, 1994b], the Variscan belt of Sardinia is arranged in three tectono-metamorphic zones: (i) an Inner Zone in the NE, which is highly deformed by medium to high-grade metamorphic events, (ii) a tectonic Nappe Zone in south-eastern and central Sardinia, characterized by greenschist metamorphism, and (iii) a Foreland Zone in the SW, characterized by very low-grade metamorphism.

Collisional deformation and crustal thickening in the shortened orogenic wedge were succeeded by tectonic inversion and extension associated with plutonism, high temperature/low pressure (HT/LP) metamorphism, exhumation of deep tectonic units, and the development of Late Carboniferous-Permian basins [*Funedda and Oggiano*, 2009]. The emplacement of the Corsica-Sardinia Batholith was associated with this late orogenic tectono-metamorphic evolution [*Poli et al.*, 1989; *Carmignani et al.*, 1994b; *Paquette et al.*, 2003; *Cocherie et al.*, 2005; *Casini et al.*, 2012].

Different mechanisms responsible for the observed postcollisional extension and tectonic unroofing have been discussed by *Conti et al.* [1999]. These include: (i) gravitational adjustment of an unstable orogenic wedge [*Platt*, 1986], (ii) slab breakoff [*Davies and von Blanckenburg*, 1995], and (iii) convective removal of mantle lithosphere [*Platt and England*, 1994]. All these models maintain high surface elevation during

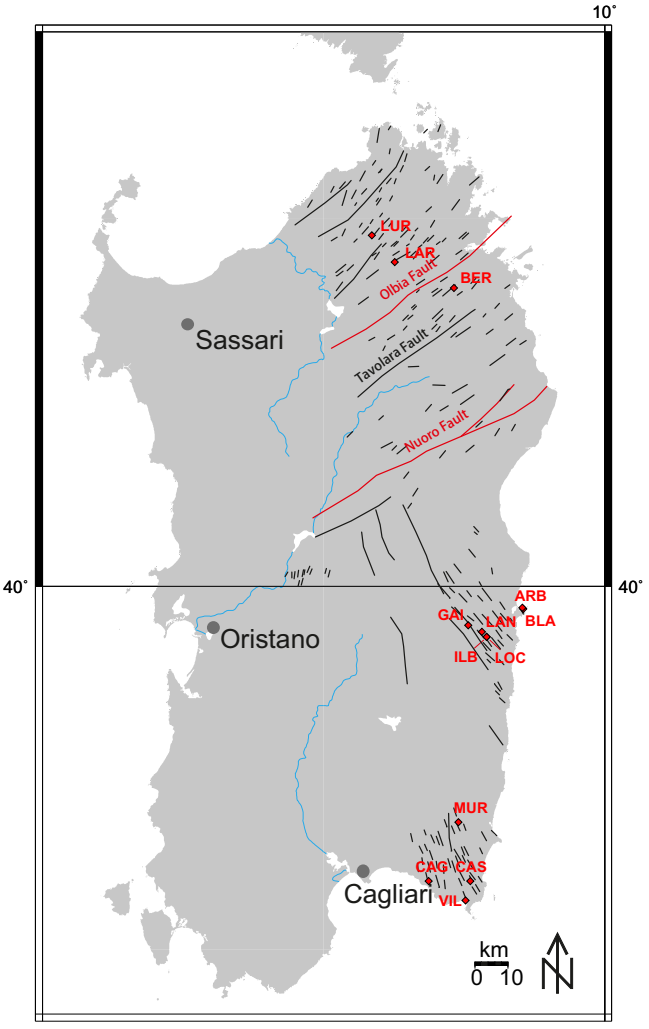

Figure 2. Location of the sampling sites of this study.

extension and should be accompanied by the formation of thick molasse basins, which, however, are lacking in the sedimentary record of Sardinia [*Conti et al*., 1999]. In any case, the progressive development of an extensional-transtensional regime is likely to have favored magma ascent and the subsequent intrusion of the Late Paleozoic dyke complexes [*Gaggero et al*., 2007].

Dyke ages have been reported to vary from Late Carboniferous in the south to Early Triassic in the north [*Baldelli et al*., 1985; *Vaccaro et al*., 1991; *Traversa and Vaccaro*, 1992; *Traversa et al*., 2003; *Atzori et al*., 2000; *Gaggero et al*., 2007]. These age data were obtained with different radiometric methods, each with inherent uncertainties. In any case, we stress that magmatic activity in post-Variscan Europe, to which Sardinia belonged, started in the Late Carboniferous, and peaked in the Early Permian (Cisuralian) [e.g., *Wilson et al*., 2004, and references therein]. To our account, there is no clear evidence of Late Permian or Early to Middle Triassic magmatism in central-southern Europe, and we therefore speculate that the radiometric ages of Sardinian dykes younger than Early Permian are due to reopening of the radiometric systems and/or analytical uncertainties.

After an overall evaluation of the available geochronological ages, we follow *Vaccaro et al*. [1991] who show the existence of two main age windows of dyke intrusion based on Rb/Sr analyses of 14 whole-rock samples and nine micas as well as 6 Ar/Ar analyses on hornblende, muscovite, and K-feldspar crystals. The resulting uncertainty of the Rb/Sr ratio is 1.5%, as determined from reproducibility tests. These analyses show that (i) in south-eastern and central-eastern Sardinia, peraluminous and high initial Sr (Sr_i) calcalkaline dykes intruded from 298 ± 5 to 289 ± 4 Ma, while (ii) further to the north (Gallura), dyke evolution ranged from peraluminous between 282 ± 4 and 268 ± 4 Ma, to low Sr_i calcalkaline at 270 ± 10 Ma.

Atzori and Traversa [1986] and *Atzori et al*. [2000] presented complementary geochronological data of dykes from central and eastern Sardinia. Their Rb/Sr ages obtained on biotite whole-rock pairs span from 291 ± 3 to 271 ± 3 Ma, in broad agreement with *Vaccaro et al*. [1991].

Structurally, we identified three different dyke provinces based on predominant strike directions. These are (i) the northern part of Sardinia, where most of the dykes strike NE-SW, (ii) the central-eastern part of Sardinia, where dykes strike preferentially NW-SE, and (iii) the south-eastern part of Sardinia, which is dominated by NNW-SSE striking dykes (Figure 2).

We sampled 13 dykes within these regions (Table 1). Four dykes were sampled in south-eastern Sardinia (CAG, CAS, MUR, and VIL; Table 1). These dykes belong to the older peraluminous suite dated from 298 ± 5 to 289 ± 4 Ma [*Vaccaro et al*., 1991]. Six dykes were sampled in the central-eastern part of Sardinia along

Table 1. Geographic Coordinates and Paleomagnetic Data of the Dykes From This Study

Site[a]	GLat	GLon	Strike (in ° cw from N)	Age (Ma)	$D°$	$I°$	k	α_{95}	N/N′	PLat°	PLon°
LUR	N40°57.2′	E9°10.3′	10–30		141.2	−5.9	37.2	5.6	19/24	38.4	242.2
BER	N40°48.7′	E9°27.8′	10		124.6	4.4	16.3	15.4	7/14	23.9	253.5
LAR	N40°52.9′	E9°15.2′	60		133.5	−2.0	39.3	8.3	9/14	32.1	248.2
Northern Sardinia			NE-SW to NNE-SSW	282 ± 4 to 268 ± 4	133.1	−1.2	68.7	15.0	3/3	31.5	247.9
							K=86.68	$A^b_{95} = 8.68°$		−43.3[c]	321.3[c]
ARB	N39°56.3′	E9°42.6′	345		90.6	−7.4	39.3	7.8	10/17	2.8	282.2
GAI	N39°53.6′	E9°30.9′	??		104.8	−18.4	38.9	8.4	9/9	17.4	277.4
ILB	N39°51.7′	E9°34.8′	320		80.6	12.2	41.5	7.6	10/24	−11.2	280.8
LOC	N39°51.7′	E9°34.8′	330		92.9	−16.2	293.2	3.9	6/9	7.5	284.1
LAN	N39°52.5′	E9°33.8′	280		91.9	14.0	10.9	17.5	8/14	−3.1	272.9
BLA	N39°56.5′	E9°42.4′	330–340		91.2	−12.3	45.5	5.5	16/16	4.9	283.7
Central-eastern Sardinia			NW to SE	298 ± 5 to 289 ± 4	91.9	−4.8	25.3	13.6	6/6	3.0	280.1
							K=58.62	$A^b_{95} = 7.47°$		−52.7[c]	24.0[c]
CAG	N39°11.3′	E9°22.4′	350–360		80.1	−16.6	37.2	6.3	15/23	−2.2	292.2
CAS	N39°11.3′	E9°31.3′	330		77.1	−41.8	31.6	7.5	13/13	5.7	306.1
MUR	N39°21.1′	E9°28.8′	345–350		85.3	6.1	34.1	6.6	15/24	−5.6	280.1
VIL	N39°08.1′	E9°30.3′	0–10		76.5	−29.5	121.0	2.3	32/42	−0.1	300.2
South-eastern Sardinia			NW-SE to N-S	298 ± 5 to 289 ± 4	80.0	−20.6	15.4	24.2	4/4	−0.9	294.0
							K=44.38	$A^b_{95} = 10.51°$		−54.9[c]	48.2[c]

[a]GLat/GLon: Geographic latitude/longitude of sampling site; Strike: refers to the strike of the dykes measured in ° clockwise from North; $D°/I°$: Paleomagnetic declination/inclination; α_{95}: circle of 95% confidence; N/N′: number of specimens used in the calculation of the mean data/number of measured specimens; PLat/PLon: latitude/longitude of the virtual geomagnetic poles and regional paleomagnetic poles.

[b]The A_{95} values for the paleomagnetic poles are well within the limits defined by *Deenen et al.* [2011] for data sets, which reliably average out paleosecular variation, which are 7.73–41.04° for three sites as in northern Sardinia, 5.86–26.52° for six sites as in central-eastern Sardinia, and 6.89–34.24° for four sites as in south-eastern Sardinia.

[c]Paleomagnetic South poles after rotation to European coordinates using rotation parameters after *Gattacceca et al.* [2007] (rotation pole coordinates $\lambda = 43.50°$, $\phi = 9.50°$, angle 45.00° cw) in order to close the Ligurian ocean and *Gong et al.* [2008] (rotation pole coordinates $\lambda = 43.00°$, $\phi = -2.00°$, angle 35.00° cw) to account for the opening of the Bay of Biscay.

the Gulf of Orosei (ARB, GAI, ILB, LOC, LAN, and BLA; Table 1). These dykes as well as the three dykes sampled at sites LUR, LAR, and BER in northern Sardinia (Table 1) consist of calc-alkaline, high-K low-Si andesites, and peraluminous ultra-acid rhyolites dated by *Atzori et al.* [2000] from 291 ± 3 to 271 ± 3 Ma.

3. Field and Laboratory Methods

All samples were taken using a gasoline-powered, water-cooled drill, and oriented using a standard magnetic compass. Subsequently, samples were cut into standard 11 cc cylindrical specimens. All samples were studied in the paleomagnetic laboratory of the University of Munich. The majority of the specimens was thermally demagnetized using a Schoenstedt furnace adopting increments of 30°C up to maximum temperatures of 690°C. Demagnetization measurements using alternating field (AF) demagnetization were also carried out using steps of 5 mT up to a maximum field of 90 mT. The AF demagnetization experiments were carried out using the automatically operated system running in the paleomagnetic laboratory of the University of Munich [*Wack and Gilder*, 2012]. The results of the AF experiments support the data obtained by thermal demagnetization (Figure 3). After each heating step or increase in alternating field strength, the natural remanent magnetization was measured with a 2 G Enterprises Superconducting Quantum Interference Device (SQUID) cryogenic magnetometer located in a magnetically shielded room. Rock-magnetic parameters were determined using a variable field translation balance [*Krása et al.*, 2007] (Figure 4). Demagnetization results were plotted on orthogonal vector diagrams [*Zijderveld*, 1967] and analyzed using the least square method [*Kirschvink*, 1980] on linear portions of the demagnetization paths defined by at least four consecutive demagnetization steps. The linear fits were anchored to the origin of the demagnetization axes where appropriate.

Each dyke is represented by one sampling site comprising between a minimum of 6 and a maximum of 42 measured samples, for a total of 13 sites and 243 samples (Table 1). Site mean directions were calculated using the paleomagnetic software of *Maier* [1998], and were used to calculate regional mean directions according to geographic distribution. This results in three regional mean directions for northern, central-eastern, and south-eastern Sardinia, based on three, six, and four site mean directions, respectively (Table 1).

The sampling strategy in this study was designed to average out paleosecular variation (PSV) as completely as possible. To ensure the recording of sufficient cooling time, samples were taken from different positions

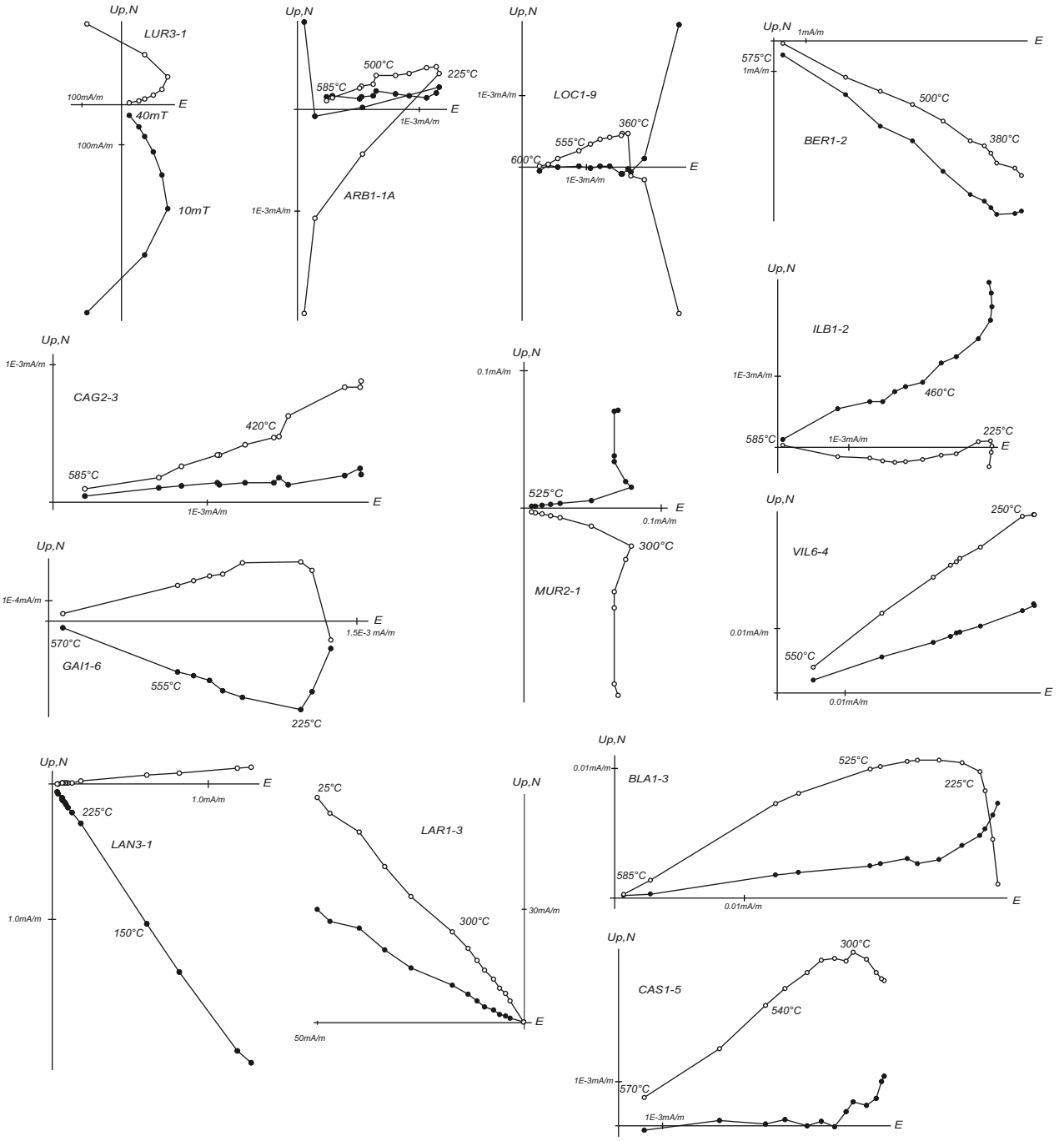

Figure 3. Results of thermal and alternating field demagnetization experiments plotted as orthogonal vector diagrams in geographic (*in situ*, IS) coordinates. Solid and open dots represent the vector endpoints projected onto the horizontal and vertical planes, respectively.

within the dykes, i.e., close to the margins as well as in the central parts. The between site scatter is indicative of successful sampling of PSV. The A_{95} values of the paleomagnetic poles (Table 1) resulted well within the intervals designed to indicate successful averaging-out of PSV for the number of sites contributing to the paleomagnetic poles, according to the criteria of *Deenen et al.* [2011] (7.73° to 41.04° for three sites as in northern Sardinia, 5.86° to 26.52° for six sites as in central-eastern Sardinia and 6.89° to 34.24° for four sites as in south-eastern Sardinia).

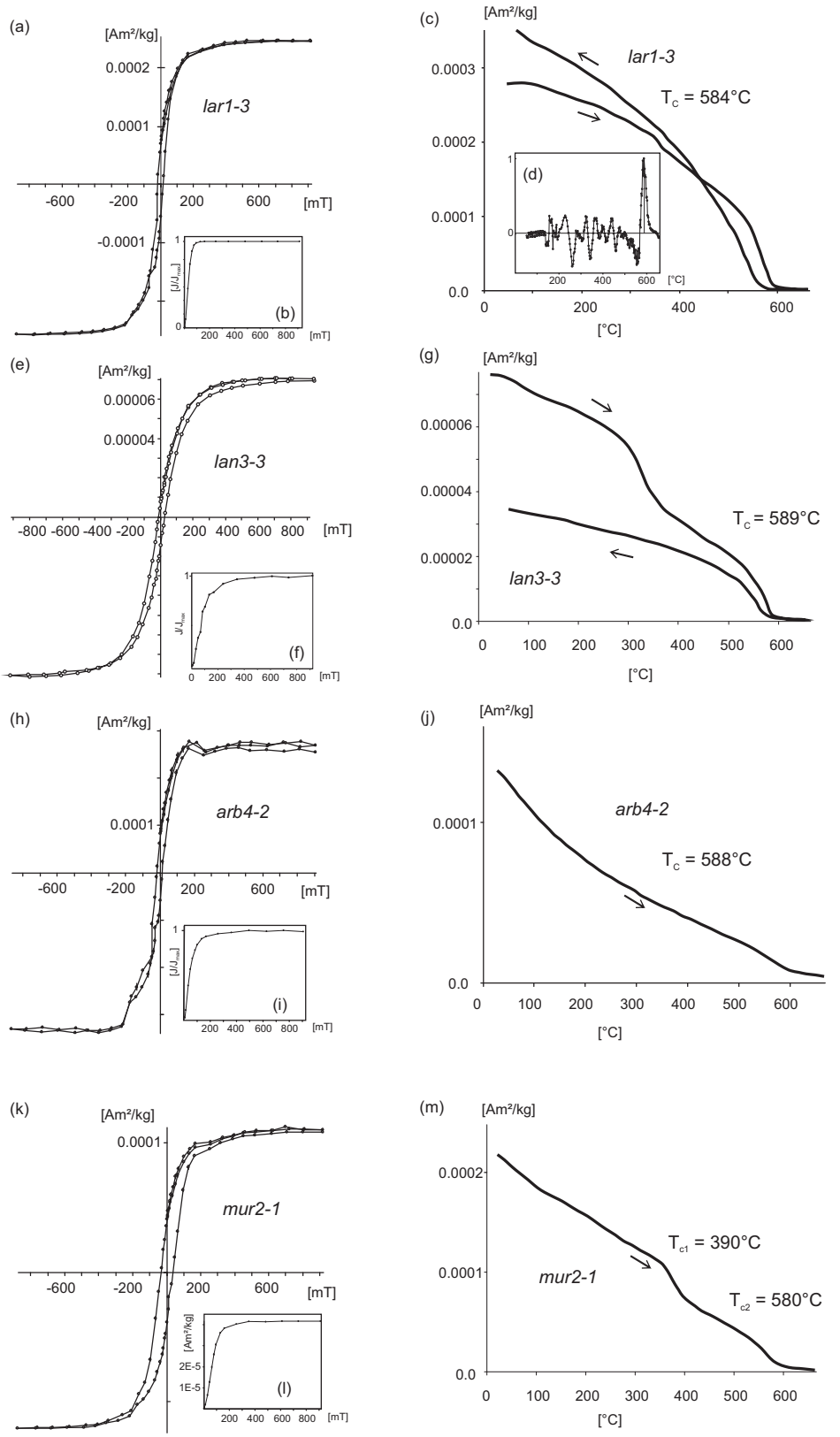

Figure 4. Rock-magnetic experiments on representative dyke samples from Sardinia. (a, e, h, k) Hysteresis loops, (b, f, i, l) IRM acquisition curves, (c, g, j, m) thermomagnetic curves, and the (d) second derivative of the heating portion of the thermomagnetic curve. [J/J_{max}]: normalized magnetization intensities and [Am^2/kg]: absolute magnetization intensities.

4. Rock-Magnetic Data

Rock-magnetic analyses include hysteresis measurements, isothermal remanent magnetization (IRM) acquisition in fields up to 700 mT, backfield magnetization for the definition of the coercivity of remanence, and, finally, in-field heating (up to 700°C) and cooling cycles (hereafter, referred to as thermomagnetic measurements) in order to estimate the Curie temperatures of the magnetic minerals (either using the method described by *Moskowitz* [1981] or the second derivative of the heating curves as displayed in Figure 4d), as well as to identify possible mineralogical transformations that occurred during heating. The hysteresis loops and the thermomagnetic curves were corrected for diamagnetic and/or paramagnetic contributions [*Leonhardt*, 2006].

The rock-magnetic analyses on samples from site LAR in the northeastern dyke province indicate the presence of magnetite as the main carrier of the magnetic remanence: the hysteresis curves and the IRM acquisition curve display saturation below 200 mT (Figures 4a and 4b), and the thermomagnetic heating curve (Figure 4c) shows a Curie temperature of 584°C (calculated after *Moskowitz* [1981]). Magnetite with an estimated Curie temperature of ~589°C is also present in samples from sites LAN and ARB from the central-eastern dyke province (Figures 4e–4j). Samples from site MUR located in the south-eastern dyke province show IRM acquisition curves that saturate at around 375 mT, while the thermomagnetic curves show a two-step decrease in magnetization intensity at ~390°C, which could be attributed to titanomagnetite, and at ~580°C, indicating that magnetite is the main carrier of the magnetic remanence in these samples (Figures 4k–4m).

5. Paleomagnetic Data

After removal of a viscous magnetic overprint at ~50°C, low temperature (LT) component directions have been observed up to 200 − 250°C in about one third of the samples. These LT components, plotted on a stereographic projection (Figure 6), yield a mean value of Dec = 1.1°E, Inc = 57.1° (N = 84, k = 22.0, α_{95}=3.3°), in broad agreement with the time averaged geomagnetic field for a nominal point in central Sardinia (Inc = 59.2°).

These LT overprint components are followed by characteristic high temperature (HT) remanent magnetization (ChRM) component directions, as will be described in the following paragraphs for the various sampled regions.

5.1. Northern Sardinia

The three dykes sampled in northern Sardinia (LUR, LAR, BER; Figure 2) yielded a total of 52 measured samples, 35 of which gave interpretable paleomagnetic results. After removal of the low temperature present-day field overprint (see above and Figure 6), high temperature component directions pointing E-SE with shallow positive or negative inclinations were identified and used to calculate site mean directions, which were then averaged to calculate a regional mean direction for northern Sardinia of Dec = 133.1°E, Inc = −1.2° (N = 3, k = 68.7, α_{95} = 15.0°; Figure 5 and Table 1). We note that two samples from site LAR show NW and up-pointing high temperature component directions, which clearly deviate from the shallow E-SE overall mean direction from northern Sardinia (Figure 3). These component directions of dubious origin were excluded from further calculations.

5.2. Central-Eastern Sardinia

The six dykes sampled in central-eastern Sardinia (ARB, GAI, ILB, LOC, LAN, and BLA; Figure 2) yielded a total of 89 measured samples, 59 of which gave useful results. As for the northern Sardinia samples, a low temperature present-day field overprint was removed up to 200 − 250°C (Figure 6) in about one third of the samples. At higher temperatures, HT component directions have been identified and used to calculate site mean directions pointing E with positive and negative inclinations ranging from −18.4° to 14.0° (Figure 3); these site mean directions were then averaged to calculate a regional mean direction for central Sardinia of Dec = 91.9°E, Inc = −4.8° (N = 6, k = 25.3, α_{95} = 13.6°; Figure 5 and Table 1). The large scatter of site mean inclinations could be due to postemplacement tilting of some dykes, e.g., dyke LAN, which has a strike direction different from the average direction of dykes in this area. Given,

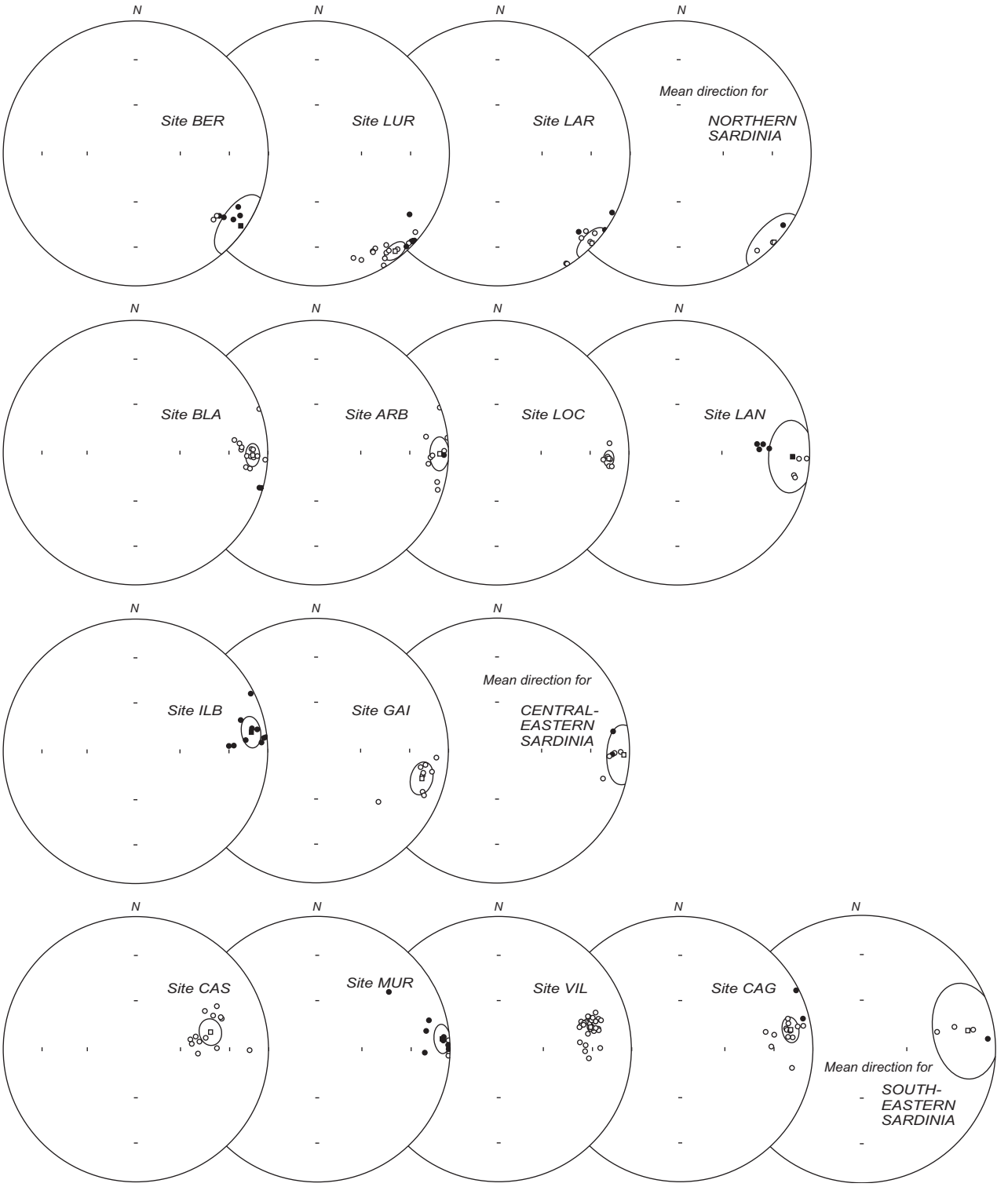

Figure 5. Stereographic projections in geographic (*in situ*, IS) coordinates of the high temperature magnetic component directions of samples from this study. Solid and open dots represent the projections on the upper and lower hemispheres, respectively. Solid and open rectangles indicate the site mean directions with 95% confidence circles (α_{95}). From the site mean directions, regional mean directions were calculated for northern, central-eastern, and south-eastern Sardinia, which are also plotted with 95% confidence circles.

however, that the site mean declinations show a reduced scatter and are statistically indistinguishable, we are confident that the analysis of vertical axis rotations is not sensibly affected by the large scatter of inclinations.

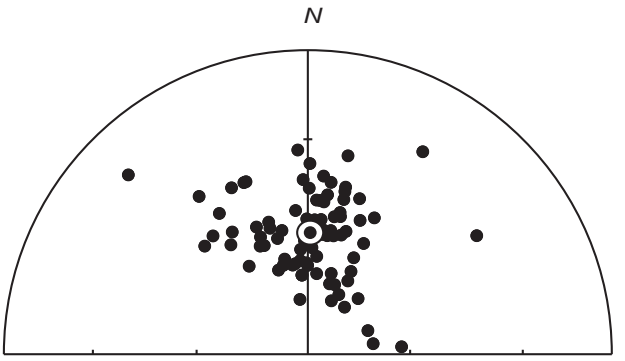

Figure 6. Stereographic projection in geographic (*in situ*, IS) coordinates of the low temperature magnetic component directions of samples from this study pointing in the direction of the Earth's present day field. The mean direction with associated 95% confidence circle (α_{95}) is also indicated.

5.3. South-Eastern Sardinia

The four dykes sampled in south-eastern Sardinia (CAG, CAS, MUR, and VIL; Figure 2) yielded of a total of 102 measured samples, 75 of which gave useful results. After removal of the present-day field overprint (Figure 6), HT component directions were isolated (Figure 3) and again averaged to calculate site mean directions pointing E-NE with positive and negative inclinations ranging from $-41.8°$ to $6.1°$ and a regional mean direction for south-eastern Sardinia of Dec = 80.0°E, Inc = $-20.6°$ (N = 4, k = 15.4, $\alpha_{95} = 24.2°$; Figure 5 and Table 1).

We note that samples from site CAS show quite steeply dipping magnetic component directions with negative inclinations on the order of $40 - 50°$. This might be the result of undetected local tilt of the sampled dyke. However, since the strike direction of dyke CAS is in broad agreement with the overall striking of dykes in south-eastern Sardinia, and since its mean magnetic component declination of $77.1°$ is statistically indistinguishable from the mean declinations of the other sites in south-eastern Sardinia, we are confident that the sampled dyke was not rotated independently, and we therefore include it in the calculation of the overall mean direction of south-eastern Sardina.

5.4. Data Summary and Comparison With Data From the Literature

The ChRM component directions found in the sampled dykes show shallow (negative or positive) inclinations and easterly or south-easterly declinations (Figure 5). We note that two sites in south-eastern Sardinia give rather high inclinations of $-41.8°$ (CAS) and $-29.5°$ (VIL). However, data from these sites have been retained because rock-magnetic and paleomagnetic measurements provide no reason to discard them. Consequently, the regional mean direction for the south-eastern sites displays a large limit of 95% confidence (24.2°) compared to the regional means of sites from northern and central-eastern Sardinia.

The data presented here for northern Sardinia (mean Dec = 133.1°E, Inc = $-1.2°$) are similar to the mean direction of Dec = 132.7°E, Inc = $-1.6°$ obtained by *Vigliotti et al.* [1990] from 11 Upper Paleozoic dykes outcropping in northern Sardinia, as well as to data obtained by *Edel et al.* [1981] from ignimbrites outcropping in NW Sardinia (Nurra) (mean Dec = 126.0°E, Inc = $-1.0°$), and dated at 296 ± 9 Ma using K-Ar on biotite crystals. Our data from northern Sardinia are also consistent with data of *Vigliotti et al.* [1990], who conducted paleomagnetic analyses on 12 Upper Paleozoic dykes in southern Corsica, and concluded that southern Corsica and northern Sardinia behaved as a single crustal block with a mean paleomagnetic direction of Dec = 133.7°E, Inc = $-6.5°$.

Our regional mean directions for central-eastern and south-eastern Sardinia of Dec = 91.9°E, Inc = $-4.8°$ and Dec = 80.0°E, Inc = $-20.6°$, respectively, are broadly similar to the mean direction of Dec = 85.0°E, Inc = $-7.0°$ obtained by *Edel et al.* [1981] on 28 ignimbrite and andesite sites from south-eastern Sardinia dated to 310–280 Ma using different K-Ar clocks [*Edel et al.*, 1981].

From the analysis illustrated above, it appears that significant relative rotations occurred between northern Sardinia-southern Corsica and central-eastern Sardinia, while minor rotations occurred between central-eastern Sardinia and south-eastern Sardinia.

6. Data Interpretation

From the distribution of site mean virtual geomagnetic poles, a paleomagnetic pole was determined for each of the three investigated dyke provinces (Table 1). These paleomagnetic poles were then restored to European coordinates using rotation parameters of *Gattacceca et al.* [2007] ($\lambda = 43.50°$, $\varphi = 9.50°$, angle 45.00° clockwise) in order to account for the opening of the Ligurian-Provençal Basin and of *Gong et al.*

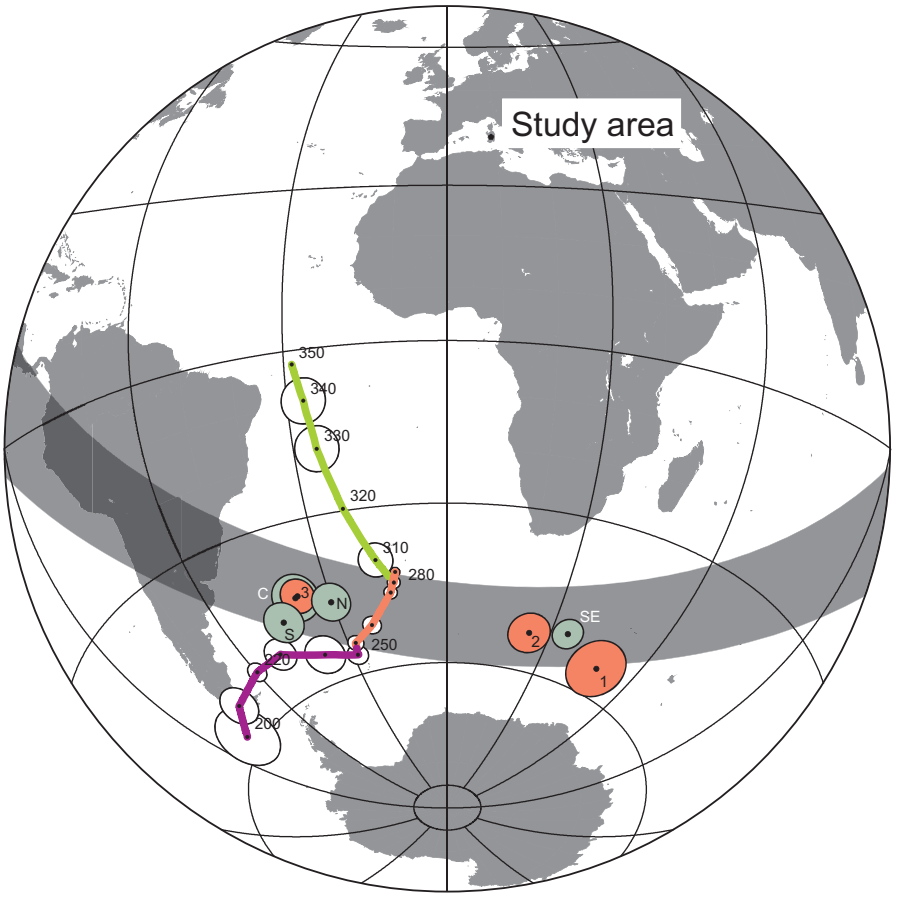

Figure 7. Paleomagnetic poles from this study for (1) south-eastern, (2) central-eastern, and (3) northern Sardinia (red with numbers attached) compared to poles from the literature (green): *Edel et al.* [1981] for southeast Sardinia (SE) and Nurra (N) and *Vigliotti et al.* [1990] for Sardinia (S) and Corsica (C). All poles are shown in European coordinates, i.e., they have been corrected for the opening of the Ligurian Ocean and the Bay of Biscay (see text for explanation). These poles plot within a small circle band centered on the 250–280 Ma time window of the Baltica apparent polar wander path of *Torsvik et al.* [2012] (solid circles with ages attached; this figure only shows the Carboniferous to Triassic/Jurassic segments of the APW path). The pole of rotation to the small circles (solid polygon) lies within Sardinia (study area) indicating true vertical axis rotations between northern and central-southern Sardinia.

[2008] ($\lambda = 43.00^\circ$, $\varphi = -2.00^\circ$, angle 35.00° clockwise) to account for the opening of the Bay of Biscay, giving a total (cumulative) rotation pole of $\lambda = 41.93^\circ$, $\varphi = 4.61^\circ$, angle 79.78° clockwise (Table 1).

To assess the relative amount of rotational displacement of crustal blocks, the restored poles have been compared to the apparent polar wander path (APWP) of Baltica [*Torsvik et al.*, 2012]. Inspection of Figure 7 reveals that the poles from this study as well as those of *Edel et al.* [1981] and *Vigliotti et al.* [1990] are strung out along a small circle band cutting the 250–280 Ma segment of the APWP of Baltica, in broad agreement with the mean ages of dyke emplacement [*Vaccaro et al.*, 1991; *Atzori et al.*, 2000; *Gaggero et al.*, 2007]. A single Euler pole of rotation, calculated as the pole to the small circle best fitting the paleomagnetic poles, can account for the differential block rotations observed; this Euler pole lies in Sardinia at latitude = 40.3°N, longitude = 8.9°E (Figure 7, small polygon). The apparent discrepancy between the older dyke poles and the younger APWP segment onto which they seem to converge could be due to uncertainties associated with radiometric dating of the dykes as well as potential errors in the Baltica APWP arising from the time-averaging of paleopoles that are not always sufficiently well dated. Alternatively, this apparent discrepancy could be due to (undetected) block tilting after dykes emplacement. In any case, we are confident that our analysis supports the successful isolation of primary magnetic component directions in the studied dykes, and also the assumption that the number of sites/samples used to calculate the mean paleomagnetic poles is sufficient to average out secular variations of the Earth's field at the time of dykes cooling (see section 3).

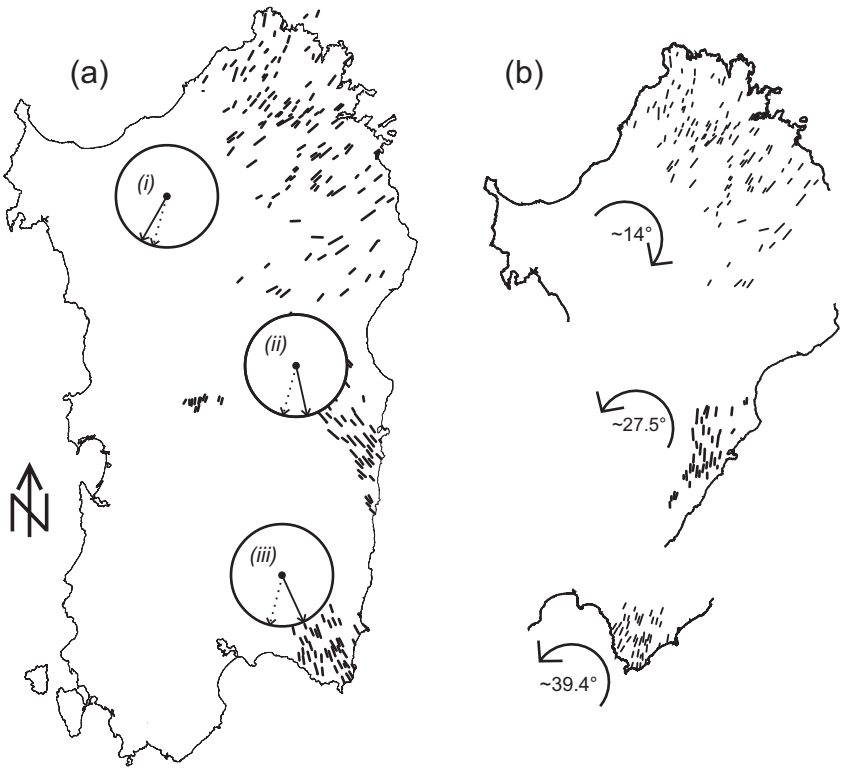

Figure 8. (a) Sardinia in its present outline and orientation with the distribution of Early Permian dyke provinces. Stippled arrows: expected Permian declinations for nominal points in (i) northern Sardinia, (ii) central-eastern Sardinia, and (iii) south-eastern Sardinia calculated from the 270 Ma pole from the Baltica AWPW of *Torsvik et al*. [2012]. Solid arrows: observed paleomagnetic declinations of the Early Permian dykes of this study. All declinations are in European coordinates (e.g., corrected for the opening of the Bay of Biscay and of the Liguro-Provençal Basin). (b) Paleogeography of Sardinia restored using the observed paleomagnetic declinations; the arrows indicate the amount and sense of rotation since the magnetization was acquired; see text for discussion.

In order to estimate the rotations of northern, central-eastern, and south-eastern Sardinia relative to the 270 Ma paleopole of Baltica of *Torsvik et al*. [2012], we restored these regions to European coordinates using the rotation parameters of *Gattacceca et al*. [2007] and *Gong et al*. [2008] (see also above), obtaining a position for a nominal point in the central part of northern Sardinia of Lat = 38.28°N, Long = 4.24°E, for a nominal point in the central part of central-eastern Sardinia of Lat = 37.81°N, Long = 3.08°E, and for a nominal point in the central part of south-eastern Sardinia of Lat = 37.74°N, Long = 2.32°E. These restored coordinates were then used to calculate the declinations and inclinations expected from the paleomagnetic poles obtained from this study, again rotated to European coordinates. The resulting directions are: Dec = 209.7°E, Inc = −0.8° for northern Sardinia, Dec = 167.5°E, Inc = −4.6° for central-eastern Sardinia, and Dec = 155.2°E, Inc = −20.5° for south-eastern Sardinia. The expected directions for the different parts of Sardinia (restored to Europe) calculated from the 270 Ma paleopole of Baltica [*Torsvik et al*., 2012] are Dec = 195.7°E, Inc = −5.1° for northern Sardinia, Dec = 195.0°E, Inc = −3.7° for central-eastern Sardinia and Dec = 194.6°E, Inc = −3.3° for southeast Sardinia, which implies differences in declinations of 14° counter-clockwise for northern Sardinia, 27.5° clockwise for central-eastern Sardinia, and 39.4° clockwise for south-eastern Sardinia. After rotation, the declinations coincide and the dyke provinces show better alignment (Figure 8). This indicates continuity of the tensional regime across large parts of the Corsica-Sardinia-Batholith during the emplacement of the dyke swarm and a coherent stretching direction. An earlier study by *Gattacceca et al*. [2004] suggests a NW-SE oriented stretching direction during dyke intrusion (*N*140°E in present day coordinates), which is coherent with the overall strike of dykes observed in our reconstruction.

7. Discussion

The observed rotations confirm and further substantiate previous paleomagnetic analyses from Permian and Carboniferous rocks of Sardinia [*Zijderveld et al*., 1970; *Edel et al*., 1981; *Edel*, 2000; *Moser*, 2004; *Moser*

et al., 2005] that reveal the existence of a complex tectonic history characterized by large-scale differential rotations of crustal blocks.

Regarding the age and tectonic significance of the observed rotations, already in the 1980s, *Edel et al*. [1981] inferred that the rotations between northern and southern Sardinia were due to an "[. . .] important phase of deformation in Late Variscan times [. . .]." Subsequent analyses confirmed and better substantiated this conclusion. *Kirscher et al*. [2011] analyzed a total of 280 samples from 44 sites of Middle and Late Jurassic age from Sardinia (Nurra, Baronie-Supramonte, Barbagia-Sarcidano, and Sulcis), obtaining site mean directions and paleomagnetic poles that indicate negligible amounts ($\pm 10^{\circ}$) of post-Jurassic internal rotations within Sardinia. We therefore exclude that the rotations described in this study are related to tectonic processes postdating the Jurassic, such as extensional tectonics affecting the European margin during the Jurassic [*Zattin et al*., 2008], Alpine tectonics that started roughly during the Late Cretaceous [*Carmignani et al*., 1994a; *Rosenbaum et al*., 2002] or transcurrent tectonics in the Cenozoic [*Carmignani et al*., 1994a; *Pasci*, 1997; *Oggiano et al*., 2009]. Moreover, Cenozoic subduction rollback tectonics cannot be held responsible for the observed rotations or the curvature of the Gulf of Orosei as proposed by *Helbing et al*. [2006a, 2006b] based on the paleomagnetic data of *Kirscher et al*. [2011] documenting the internal coherence of Sardinia in post-Jurassic times. This opens the possibility that the observed rotations could have occurred during the Permian after the Variscan coalescence of Gondwana and Laurasia.

The block rotations documented in this study are reminiscent of block rotations previously observed in Permian and Triassic sediments and volcanic rocks from the Toulon-Cuers basin of SE France [*Aubele et al*., 2012], which was located along the European margin immediately to the west of Sardinia in Permian times. Similarly to what is observed in this study, the latitudes of the Early to Middle Permian paleopoles from Toulon-Cuers agree well with the corresponding segment of the APWP of Baltica (Europe), whereas the longitudes are strung out along a small circle segment, indicating relative rotations between the sampled regions and stable Europe. The Triassic poles, instead, plot close to the Triassic segment of the European APWP and provide a strong constraint on the age of the observed rotations, which is likely late Early-Middle Permian. To the west of Toulon-Cuers, a very similar timing of block rotations was observed in the Lodève, Brive, and Saint-Affrique basins of the French Massif Central where Early Permian rocks show rotated paleomagnetic vectors while Late Permian rocks have not been affected by rotations [*Merabet and Guillaume*, 1988; *Cogné et al*., 1990, 1993; *Diego-Orozco and Henry*, 1998; *Henry et al*., 1999; *Diego-Orozco et al*., 2002; *Chen et al*., 2006]. In addition, paleomagnetic data from the Maures-Estérel massif located immediately to the east of the study area in SE France suggest a large clockwise block rotation during the late Early to Middle Permian [*Edel*, 2000].

8. Conclusions

Paleomagnetic data collected over large parts of the western Mediterranean Variscides seem to indicate the existence of an intra-Pangea belt of tectonic blocks straddling from the Massif Central to southern France and Corsica-Sardinia characterized by complex and differential block rotations that may have largely occurred in post-Early Permian and pre-Early Triassic times. The timing of the transformation from Irving's Pangea B [*Irving*, 1977] to a Wegenerian Pangea A configuration broadly agrees with the timing of block rotation documented in this and previous studies. This postulated transformation occurred essentially during the Middle Permian from an Early Permian Pangea B to a Late Permian Pangea A [*Muttoni et al*., 1996, 2003, 2009]. The Middle Permian, therefore, seems to coincide with a period of major intra-Pangea plate reorganization associated with magmatic activity as suggested by several authors [e.g., *Deroin and Bonin*, 2003; *Isozaki*, 2009].

We have previously illustrated [*Aubele et al*., 2012] that the simple two-dimensional model developed by *McKenzie and Jackson* [1983] can explain the existence of differential (clockwise and counter-clockwise) rotations of crustal blocks within a zone of distributed deformation imposed by the relative motion of the bounding plates. Accordingly, we suggest that the various crustal blocks of Sardinia-Corsica and SE France were rotated by variable amounts and sense as they were trapped within a diffuse shear zone between Laurasia and Gondwana [e.g., *Arthaud and Matte*, 1977] active during the Permian. In this scenario, an assumed dextral shear between Laurasia and Gondwana would lead to systematic clockwise or counter-clockwise rotations about vertical axes of crustal blocks of variable shape and dimension located within the

shear zone. We speculate that the large-scale rotations of fault-bounded blocks observed in the Permian dykes of Sardinia, as well as in Permian series elsewhere in Europe, may have been induced by post-Variscan intra-Pangea wrenching and shearing occurring during Pangea instability and transformation (see *Muttoni et al.* [2003], *Aubele et al.* [2012], and *Domeier et al.* [2012] for a detailed discussion on the Pangea debate).

Our working hypothesis of continental-scale shearing between Laurasia and Gondwana occurring as a consequence of Pangea transformation during the Permian will benefit from future studies from other dyke provinces potentially caught in the shear zone, e.g., in Calabria (Sila Grande) and Catalonia.

Acknowledgments

This project has been funded by the German Science Foundation (DFG) grants BA 1210/8-1 and BA 1210/20-1. Special thanks goes to Dennis Kent whose comments on an earlier version of the paper were very helpful. We are indebted to Paola Pittau and Myriam Del Rio for fundamental help in solving burocratic problems during our sampling campaign. Special thanks goes to Barbara Emmer for help in the field and Giuseppe Muttoni for legal advice. We are also thankful for very helpful and substantial reviews provided by J. Gattacceca and C. Mac Niocaill. Access to the raw data will be provided by the authors upon request.

References

Arthaud, F., and P. Matte (1977), Late Paleozoic strike-slip faulting in southern Europe and northern Africa: Result of a right-lateral shear zone between the Appalachians and the Urals, *Geol. Soc. Am. Bull.*, *88*, 1305–1320.

Atzori, P., and G. Traversa (1986), Post-granitic permo-triassic dyke magmatism in eastern Sardinia (Sarrabus p.p., Barbagia, Mandrolisai, Goceano, Baronie and Gallura), *Period. Mineral.*, *55*, 203–231.

Atzori, P., R. Cirrincione, A. Del Moro, and P. Mazzoleni (2000), Petrogenesis of late Hercynian calc-alkaline dykes of mid-eastern Sardinia: Petrographical and geochemical data constraining hybridization process, *Eur. J. Mineral.*, *12*, 1261–1282.

Aubele, K., V. Bachtadse, G. Muttoni, A. Ronchi, and M. Durand (2012), A Paleomagnetic study of Permian and Triassic rocks from the Toulon-Cuers basin, SE France: Evidence for intra-Pangea block rotations in the Permian, *Tectonics*, *3*, TC3015, doi:10.1029/2011TC003026.

Baldelli, C., F. M. Elter, and P. Macera (1985), Segnalazione di un lamprofiro alcalino permo-triassico intruso fra i micascisti a granato-staurolite-cianite nella Sardegna NE, in Evoluzione stratigrafica, tettonica, metamorfica e magmatica del Paleozoico italiano. *Riun. Scient. Siena*, 70–71.

Burg, J. P., J. van den Driessche, and I. P. Brun (1994), Syn- to post-thickening extension in the Variscan belt of Western Europe: Modes and structural consequences, *Geol. Fr.*, *3*, 33–51.

Carmignani, L., T. Cocozza, N. Minzoni, and P. C. Pertusati (1978), The Hercynian orogenic revolution in Sardinia, *Z. Geol. Ges.*, *129*, 485–493.

Carmignani, L., S. Barca, L. Disperati, P. Fantozzi, A. Funedda, G. Oggiano, and S. Pasci (1994a), Tertiary compression and extension in the Sardinian basement, *Bol. Geofis. Teor. Appl.*, *36*, 45–62.

Carmignani, L., R. Carosi, and A. Di Pisa (1994b), The Hercynian chain in Sardinia (Italy), *Geodin. Acta*, *7*, 31–47.

Casini, L., S. Cuccuru, M. Maino, G. Oggiano, and M. Tiepolo (2012), Emplacement of the Arzachena Pluton (Corsica-Sardinia Batholith) and the geodynamics of incoming Pangaea, *Tectonophysics*, *544–545*, 31–49.

Chen, Y., B. Henry, M. Faure, J.-F. Becq-Giraudon, J.-Y. Talbot, L. Daly, and M. Le Goff (2006), New Early Permian paleomagnetic results from the Brive basin (French Massif Central) and their implications for Late Variscan tectonics, *Int. J. Earth Sci.*, *95*, 306–317.

Cocherie, A., P. Rossi, C. Fanning, and C. Guerrot (2005), Comparative use of TIMS and SHRIMP for U-Pb zircon dating of A-type granites and mafic tholeiitic layered complexes and dykes from the Corsican batholith (France), *Lithos*, *82*, 185–219.

Cogné, J. P., J. P. Brun, and J. Van den Driessche (1990), Paleomagnetic evidence for rotation during Stephano-Permian extension in southern Massif Central (France), *Earth Planet. Sci. Lett.*, *101*, 272–280.

Cogné, J. P., J. Van den Driessche, and J. P. Brun (1993), Syn-extension rotations in the Permian St. Affrique basin (Massif Central, France): Paleomagnetic constraints, *Earth Planet. Sci. Lett.*, *115*, 29–42.

Conti, P., L. Carmignani, G. Oggiano, A. Funedda, and A. Eltrudis (1999), From thickening to extension in the Variscan belt—Kinematic evidence from Sardinia (Italy), *Terra Nova*, *11*, 93–99.

Cortesogno, L., G. Cassinis, G. Dallagiovanna, L. Gaggero, G. Oggiano, A. Ronchi, S. Seno, and M. Vanossi (1998), The Variscan post-collisional volcanism in Late Carboniferous-Permian sequences of Ligurian Alps, Southern Alps and Sardinia (Italy): A synthesis, *Lithos*, *45*, 305–328.

Davies, J. H., and F. von Blanckenburg (1995), Slab breakoff: A model of lithosphere detachment and its test in the magmatism and deformation of collisional orogens, *Earth Planet. Sci. Lett.*, *129*, 85–102.

Deenen, M. H. L., C. G. Langereis, D. J. J. van Hinsbergen, and A. J. Biggin (2011), Geomagnetic secular variation and the statistics of palaeomagnetic directions, *Geophys. J. Int.*, *186*, 509–520, doi:10.1111/j.1365-246X.2011.05050.x.

Deroin, J. P., and B. Bonin (2003), Late Variscan tectonomagmatic activity in Western Europe and surrounding areas: The mid-Permian Episode, *Bol. Soc. Geol. It.*, *2*, 169–184.

Diego-Orozco, A., and B. Henry (1998), Palaeomagnetic data from the Permian Rodez basin and rotations in the southwestern border of the Massif Central, *C. R. Acad. Sci., Ser. II*, *327*, 225–229.

Diego-Orozco, A., Y. Chen, B. Henry, and J.-F. Becq-Giraudon (2002), Paleomagnetic results from the Permian Rodez basin implications: The Late Variscan tectonics in the southern French Massif Central, *Geodin. Acta*, *15*, 249–260.

Domeier, M., R. Van der Voo, and T. Torsvik (2012), Paleomagnetism and Pangea: The road to reconciliation, *Tectonophysics*, *514–517*, 14–43.

Edel, J.-B. (2000), Hypothèse d'une ample rotation horaire tardi-varisque du bloc Maures-Estérel-Corse-Sardaigne, *Geol. Fr. Géologie de la France, n° 1*, pp. 3–19.

Edel, J. B., R. Montigny, and R. Thuizat (1981), Late Paleozoic rotations of Corsica and Sardinia: New evidence from paleomagnetic and K-Ar studies, *Tectonophysics*, *79*, 201–223.

Funedda, A., and G. Oggiano (2009), Outline of the Variscan basement of Sardinia, *Rend. Soc. Paleontol. Ital.*, *3*(1), 23–35.

Gaggero, L., G. Oggiano, L. Buzzi, F. Slejko, and L. Cortesogno (2007), Post-Variscan Mafic Dikes from the late Orogenic Collapse to the Tethyan Rift: Evidence from Sardinia, *Ofioliti*, *32*(1), 15–37.

Gattacceca, J., J.-B. Orsini, J.-P. Bellot, B. Henry, P. Rochette, P. Rossi, and G. Cherchi (2004), Magnetic fabric of granitoids from Southern Corsica and Northern Sardinia and implications for Late Hercynian tectonic setting, *J. Geol. Soc.*, *161*, 277–289.

Gattacceca, J., A. Deino, R. Rizzo, D. S. Jones, B. Henry, B. Beaudoin, and F. Vadeboin (2007), Miocene rotation of Sardinia: New paleomagnetic and geochronological constraints and geodynamic implications, *Earth Planet. Sci. Lett.*, *258*, 359–377.

Gong, Z., C. G. Langereis, and T. A. T. Mullender (2008), The rotation of Iberia during the Aptian and the opening of the Bay of Biscay, *Earth Planet. Sci. Lett.*, *273*, 80–93.

Helbing, H., W. Frisch, P. D. Bons, and J. Kuhlemann (2006a), Tension gash-like back-arc basin opening and its control on subduction roll-back inferred from Tertiary faulting in Sardinia, *Tectonics*, *25*, TC4008, doi:10.1029/2005TC001904.

Helbing, H., W. Frisch, and P. D. Bons (2006b), South Variscan terrane accretion: Sardinian constraints on the intra-Alpine Variscides, *J. Struct. Geol.*, *28*, 1277–1291.
Henry, B., J.-F. Becq-Giraudon, and H. Rouvier (1999), Paleomagnetic studies in the Permian Basin of Largentière and implications for the Late Variscan rotations in the French Massif Central, *Geophys. J. Int.*, *138*, 188–198.
Irving, E. (1977), Drift of the major continental blocks since the Devonian, *Nature*, vol. 270, pp. 304–309.
Isozaki, Y. (2009), Illawarra reversal: The fingerprint of a superplume that triggered Pangean breakup and the end-Guadalupian (Permian) mass extinction, *Gondwana Res.*, *15*, 421–432.
Kirscher, U., V. Bachtadse, K. Aubele, and G. Muttoni (2011), Paleomagnetism of Jurassic Carbonate Rocks from Sardinia—No indication of Post Jurassic internal block rotations, *J. Geophys. Res.*, *116*, B12107, doi:10.1029/2011JB008422.
Kirschvink, J. L. (1980), The least-square line and plane and the analysis of paleomagnetic data, *Geophys. J. R. Astron. Soc.*, *62*, 699–718.
Krása, D., K. Petersen, and N. Petersen (2007), Variable field translation balance, in *Encyclopedia of Geomagnetism and Paleomagnetism, Encycl. of Earth Sci. Ser.*, edited by D. Gubbins and E. Herrero-Bervera, Springer, Netherlands, pp. 977–979, doi:10.1007/978-1-4020-4423-6_312.
Leonhardt, R. (2006), Analyzing rock magnetic measurements: The RockMagAnalyzer 1.0 software, *Comput. Geosci.*, *32*, 1420–1431.
Maier, F. (1998), Paläo- und gesteinsmagnetische Untersuchungen an Sedimenten aus Madagaskar. Implikationen für die Paläoposition Madagaskars und die Rekonstruktion von Pangäa, PhD thesis, Ludwig-Maximilians-Universität, Munich, Germany.
McKenzie, D. P., and J. A. Jackson (1983), The relationship between strain rates, crustal thickening, paleomagnetism, finite strain, and fault movement within a deforming zone, *Earth Planet. Sci. Lett.*, *65*, 182–202.
Merabet, N., and A. Guillaume (1988), Palaemagnetism of the Permian rocks of Lodève (Hérault, France), *Tectonophysics*, *145*, 21–29.
Morel, P., and E. Irving (1981), Paleomagnetism and the evolution of Pangea, *J. Geophys. Res.*, *86*(B3), 1858–1872.
Moser, E. (2004), Paleomagnetic study of Permian sediments and volcanic rocks from Sardinia—Testing the Pangea B Hypothesis, master's thesis, Ludwig-Maximilians Univ., Munich, Germany.
Moser, E., B. Emmer, V. Bachtadse, D. V. Kent, G. Muttoni, and A. Ronchi (2005), Paleomagnetism of Permian sediments and volcanic rocks from Sardinia, Abstract presented at 2005 Fall Meeting, GP11A-0014, AGU, San Francisco, Calif.
Moskowitz, B. M. (1981), Methods for estimating curie temperatures of titanomaghemites from experimental J_s-T data, *Earth Planet. Sci. Lett.*, *53*, 84–88.
Muttoni, G., D. V. Kent, and J. E. T. Channell (1996), Evolution of Pangea: Paleomagnetic constraints from the Southern Alps, Italy, *Earth Planet. Sci. Lett.*, *140*, 97–112.
Muttoni, G., D. V. Kent, E. Garzanti, P. Brack, N. Abrahamsen, and M. Gaetani (2003), Early Permian Pangea B to Late Permian Pangea A, *Earth Planet. Sci. Lett.*, *215*(3), 379–394.
Muttoni, G., M. Gaetani, D. V. Kent, D. Sciunnach, L. Angiolini, F. Berra, E. Garzanti, M. Mattei, and A. Zanchi (2009), Opening of the Neo-Tethys Ocean and the Pangea B to Pangea A transformation during the Permian, *GeoArabia*, *14*(4), 17–48.
Oggiano, G., A. Funedda, L. Carmignani, and S. Pasci (2009), The Sardinia-Corsica microplate and its role in the Northern Apennine. Geodynamics: New insights from the Tertiary intraplate strike-slip tectonics of Sardinia, *Ital. J. Geosci. (Bol. Soc. Geol. It.)*, *128*(2), 527–539.
Paquette, J.-L., R.-P. Ménot, C. Pin, and J.-B. Orsini (2003), Episodic and short-lived granitic pulses in a postcollisional setting: Evidence from precise U-Pb zircon dating through a crustal cross section in Corsica, *Chem. Geol.*, *198*(1–2), 1–20.
Pasci, S. (1997), Tertiary transcurrent tectonics of North-Central Sardinia, *Bull. Soc. Geol. Fr.*, *168*, 301–312.
Platt, J. P. (1986), Dynamics of orogenic wedges and the uplift of high-pressure metamorphic rocks, *Bull. Geol. Soc. Am.*, *97*, 1037–1053.
Platt, J. P., and P. C. England (1994), Convective removal of lithosphere beneath mountain belts; thermal and mechanical consequences, *Am. J. Sci.*, *294*, 307–336.
Poli, G., C. Ghezzo, and S. Conticelli (1989), Geochemistry of granitic rocks from the Hercynian Sardinia-Corsica batholith: Implication for magma genesis, *Lithos*, *23*(4), 247–266.
Rosenbaum, G., G. S. Lister, and C. Duboz (2002), Relative motions of Africa, Iberia, and Europe during Alpine orogeny, *Tectonophysics*, *359*, 117–129.
Stampfli, G. M. (Ed.) (2001), *Geology of the Western Swiss Alps*, vol. 36, pp. 1–41, Mém. Géol., Lausanne, Switzerland.
Torsvik, T. H., et al. (2012), Phanerozoic polar wander, palaeogeography and dynamics, *Earth Sci. Rev.*, *114*, 325–368.
Traversa, G., and C. Vaccaro (1992), REE distribution in the late Hercynian dikes from Sardinia, in *IGCP n 276 Newsletter*, vol. 5, pp. 241–262, Siena.
Traversa, G., S. Ronca, A. Del Moro, C. Pasquali, N. Buraglini, and G. Barabino (2003), Late to post-Hercynian dyke activity in the Sardinia-Corsica domain: A transition from orogenic calc-alkaline to anorogenic alkaline magmatism, *Bol. Soc. Geol. It.*, *2*, 131–152.
Vaccaro, C., P. Atzori, A. Del Moro, M. Oddone, G. Traversa, and I. M. Villa (1991), Geochronology and Sr isotope geochemistry of late-Hercynian dykes from Sardinia, *Schweiz. Mineral. Petrogr. Mitt.*, *71*, 221–230.
Vigliotti, L., W. Alvarez, and M. O. McWilliams (1990), No relative rotation detected between Corsica and Sardinia, *Earth Planet. Sci. Lett.*, *98*, 313–318.
Wack, M. R., and S. A. Gilder (2012), The SushiBar: An automated system for paleomagnetic investigations, *Geochem. Geophys. Geosyst.*, *13*, Q12Z38, doi:10.1029/2011GC003985.
Wilson, M., E.-R. Neumann, G. R. Davies, M. J. Timmermann, M. Heeremans, and B. T. Larsen (2004), Permo-Carboniferous magmatism and rifting in Europe: Introduction, *Geol. Soc. Spec. Publ.*, *223*, 1–10, doi:10.1144/GSL.SP.2004.223.01.01.
Zattin, M., F. Massari, and J. Médus (2008), Thermochronological evidence for Mesozoic-Tertiary tectonic evolution in the eastern Sardinia, *Terra Nova*, *20*, 469–474.
Zijderveld, J. D. A. (1967), A. C. demagnetization of rocks: Analysis of results, in *Methods in Paleomagnetism*, edited by D. W. Collinson, K. M. Creer, and S. K. Runcorn, pp. 254–286, Elsevier, Amsterdam.
Zijderveld, J. D. A., K. A. De Jong, and R. Van der Voo (1970), Rotation of Sardinia: Palaeomagnetic evidence from Permian rocks, *Nature*, *226*, 993–994.